

MOND and the More Fundamental Plane

R.H. Sanders and D.D. Land

Kapteyn Astronomical Institute, P.O. Box 800, 9700 AV Groningen, The Netherlands

received: ; accepted:

ABSTRACT

Bolton et al. (2007) have derived a mass-based fundamental plane using photometric and spectroscopic observations of 36 strong gravitational lenses. The lensing allows a direct determination of the mass-surface density and so avoids the usual dependence on mass-to-light ratio. We consider this same sample in the context of modified Newtonian dynamics (MOND) and demonstrate that the observed mass-based fundamental plane coincides with the MOND fundamental plane determined previously for a set of high-order polytropic spheres chosen to match the observed range of effective radii and velocity dispersions in elliptical galaxies. Moreover, the observed projected mass within one-half an effective radius is consistent with the mass in visible stars plus a small additional component of “phantom dark matter” resulting from the MOND contribution to photon deflection.

1 INTRODUCTION

Modified Newtonian dynamics (MOND) posits a fundamental acceleration scale (a_0) below which the law of gravity or inertia deviates from the Newtonian form (Milgrom 1983). Therefore, a generic prediction is that in systems where the internal acceleration, expressed as a surface density, exceeds a critical limit (a_0/G), there should be little discrepancy between the observable mass and the Newtonian dynamical mass. In traditional language, there should be no evidence for dark matter within high surface brightness systems.

Examples of high surface brightness systems are globular clusters and luminous elliptical galaxies. It is well-known that the standard Newtonian analysis of the internal kinematics of globular clusters yields mass-to-light ratios that are completely consistent with normal stellar populations (e.g., Pryor et al. 1989). However, dark matter proponents were surprised by the more recent analysis of planetary nebulae kinematics in several luminous ellipticals which implied a “dearth of dark matter” within the bright inner regions of these galactic systems (Romanowsky et al. 2003). This result is completely consistent with the expectations of MOND (Milgrom & Sanders 2003).

The galaxy scale lenses that produce multiple images of background sources—strong lenses—are primarily in early type galaxies: ellipticals or bulge dominated spirals (Kochanek et al. 2004); that is to say, high surface brightness systems. Because the surface density of lenses necessary to produce multiple images generally exceeds the MOND critical surface density, a MOND corollary prediction is that the implied mass surface density in strong gravitational lenses should be consistent with that of observable starlight, i.e., little or no dark matter in strong, galaxy scale, gravitational lenses, at least within the Einstein ring radius: “what you see is all there is.”

Recently, Bolton et al. (2007) have considered the “fundamental plane” of early type galaxies (the observed rela-

tion between effective radius, surface brightness and velocity dispersion) as defined by a sample of 36 strong lens galaxies from the Sloan Lens ACS. The lensing analysis was combined with spectroscopic and photometric observations of the individual lens galaxies in order to generate a “more fundamental plane” based upon mass surface density rather than surface brightness. They found that this *mass-based* fundamental plane relation exhibits less scatter and is closer to the expectations of the Newtonian virial relation than is the usual luminosity-based fundamental plane. This presumably is due to the absence of both an intrinsic scatter in M/L as well as its systematic variation with luminosity. Below, we emphasise that the implied lensing M/L values within the Einstein ring radius do not require the presence of a substantial component of dark matter, again consistent with the expectations of MOND.

With MOND, the mass-velocity dispersion ($M - \sigma$) relation (or its observational equivalent, the luminosity-based Faber-Jackson law), is, in some sense, more fundamental than the fundamental plane. In fact, near isothermal, homologous objects exhibit a precise mass-velocity dispersion relation (Milgrom 1984). But, in order to match the observed range of elliptical galaxy properties—primarily the distribution of the velocity dispersion vs. effective radius—models for such systems must deviate from strict homology. The necessary deviation yields a large scatter in the predicted $M - \sigma$ law; none-the-less, the models define a narrow mass-based fundamental plane when an additional parameter is included, such as effective radius or surface density (Sanders 2000).

Here, we compare this previously derived MOND fundamental plane to the mass-based fundamental plane of Bolton et al. Using the theoretical fundamental plane relation to calculate the mass from the observed effective radius and velocity dispersion, it is found that the projected MOND FP mass, presumably entirely baryonic, is proportional to

the observed lensing mass with only a small, and understandable, offset. Moreover, the implied MOND M/L-colour relationship for these systems is entirely consistent with population synthesis models. In other words, the MOND fundamental plane matches the observed “more” fundamental plane, and both require no additional dark matter in these high surface brightness galaxies.

2 THE MORE FUNDAMENTAL PLANE

The fundamental plane of elliptical galaxies (Dressler et al. 1987, Djorgovski & Davis 1987) is a scaling relationship involving the observed effective radius, r_{eff} , the central line-of-sight velocity dispersion, σ_0 , and, in the original form, the mean surface brightness within an effective radius, I . This is usually expressed as

$$\log(r_e) = a \log(\sigma) + b \log(I) + d \quad (1)$$

(it may alternatively be written as a relationship between total luminosity, effective radius, and velocity dispersion). The analysis of Sloan data on elliptical galaxies implies that $a \approx 1.5$ and $b \approx -0.8$ (Benardi et al. 2003), while the expectations from the Newtonian virial theorem, assuming homology and constant M/L, would be $a = 2$ and $b = -1$. The observed deviation from these expectations is generally thought to be due to systematic deviations from homology or from constant M/L.

The significant achievement of Bolton et al. was to use gravitational lensing in order to eliminate the dependence on M/L. The strong gravitational lensing provides the mass surface density within the Einstein ring radius (r_{ein}); therefore surface density, Σ , may be substituted for surface brightness in the above relationship. The Einstein ring radius in their sample is generally about half the effective radius, so the surface density is taken to be that within $r_{eff}/2$ (the correction from the r_{ein} to $r_{eff}/2$ is done either by assuming a mass distribution like that of an isothermal sphere or that light traces mass). This was then combined with spectroscopic and photometric observations of the lens galaxies to generate a “mass” fundamental plane. The resulting relation exhibits considerably less scatter and the exponents are close to the virial expectations: $a = 1.86 \pm 0.17$, $b = -0.93 \pm 0.09$, $d = 5.4 \pm 0.9$ with the mass traces light assumption (here the effective radius is in kpc, the velocity dispersion in kms^{-1} and the surface density in $\text{M}_\odot \text{kpc}^{-2}$).

In general, the Newtonian virial theorem implies that the mass within radius r is given by

$$M = c\sigma^2 r / G \quad (2)$$

where c is a constant determined by the structure of the object. Therefore Bolton et al. also express their result by plotting the mass of the lens (within $r_{eff}/2$) against a “dimensional” mass variable given by $\sigma^2 r_{eff}/(2G)$ where σ is the mean line-of-sight velocity dispersion within $r_{eff}/2$. The result of this is shown by the points in Fig. 1 which are well fit by

$$\log(M_{lens}) = \delta \log(M_{dim}) + C. \quad (3)$$

with $\delta = 0.98$ and $C \approx 0.6$. Therefore, these observations are consistent with the Newtonian virial theorem and no variation of the structure constant; elliptical galaxies would

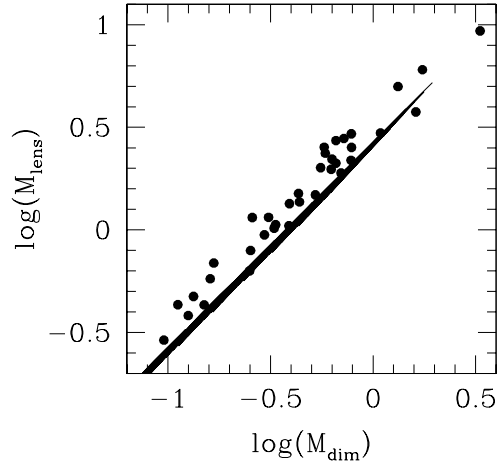


Figure 1. The points illustrate the mass-based fundamental plane of Bolton et al. (2007) shown as a relation between the observed projected mass within $r_{eff}/2$ and the dimensional mass (eq. 2). Also shown is the same for the MOND fundamental plane as determined from 360 anisotropic high order polytropes (Sanders 2000).

appear to be quite homologous over a wide range of mass. Moreover, the implied M/L values (r-band) for these galaxies range from about two to eight in solar units and are somewhat higher than predicted by population synthesis models (Fig. 3, upper panel). This point is addressed further below, but, overall, for early-type galaxies M/L values in this range would not constitute compelling evidence for dark matter within $r_{eff}/2$.

3 THE MOND FUNDAMENTAL PLANE

By solving the structure equation, Milgrom (1984) has demonstrated that, with MOND, isothermal spheres with a fixed degree of anisotropy have finite mass, an upper limit to the surface density ($\approx a_0/G$) and exhibit a $M - \sigma^4$ relationship (the basis of the Faber-Jackson law); therefore, such objects might constitute sensible models for elliptical galaxies. However, the observed properties of ellipticals—in particular, their distribution and scatter on the σ_0 - r_{eff} plane (Jørgensen 1999; Jørgensen, Franx & Kærgard 1995a; Jørgensen, Franx & Kærgard 1995b)—cannot be matched by isothermal spheres or any strictly homologous class of objects. The MOND isothermal sphere is too inflated for a given velocity dispersion—the mean surface density within an effective radius is too low. In order to match these observed properties of elliptical galaxies with MOND, it is necessary to exploit other degrees of freedom: models must deviate from being strictly isothermal with a fixed degree of orbital anisotropy.

In order to explore these possible degrees of freedom, Sanders (2000) has considered high order polytropic spheres

with an anisotropy parameter, $\beta = 1 - \sigma_t^2/\sigma_r^2$, which varies systematically with radius as in the Osipkov-Merritt models, $\beta = r^2/(r^2 + r_a^2)$, (r_a is the anisotropy radius, Binney & Tremaine 1987). For a polytropic sphere of index n the radial velocity dispersion-density relationship is given by

$$\sigma_r^2 = A\rho^{1/n} \quad (4)$$

where A is a constant ($n \rightarrow \infty$ corresponds to the isothermal sphere). It was found that a range $12 < n < 16$ was sufficient to match the the mean value and wide dispersion of effective radius for a given velocity dispersion, provided that the anisotropy radius also varies over the range $2 < r_a/r_{eff} < 25$. The luminosity or mass density distribution within these objects is similar to that of a Jaffe model (Jaffe 1982): within roughly r_{eff} the density falls as r^{-2} and beyond steepens to r^{-4} . Spherically symmetric N-body calculations with MONDian modified gravity (Bekenstein & Milgrom 1984) demonstrate that object resembling these high-order polytropes may actually condense and recollapse out of the Hubble flow (Sanders 2008).

Each model, characterised by a particular value of n and r_a/r_{eff} , exhibits its own exact $M \propto \sigma^4$ relationship but for all models combined there is a large dispersion in this relation. None-the-less, in spite of the dispersion in homology, the models lie on a narrow fundamental plane.

$$\log(r_e) = 2.0 \log(\sigma_{e2}) - 1.06 \log(\Sigma_{e2}) + 6.16 \quad (5)$$

where σ_{e2} and Σ_{e2} are the velocity dispersion and the average surface density respectively within $r_{eff}/2$ (the coefficients here differ slightly from those given by Sanders because of scaling to $r_{eff}/2$). This is seen to be quite close to the Newtonian virial expectation and within the errors of the more fundamental plane defined by the gravitational lenses. The set of anisotropic polytropes may also be replaced by isotropic Jaffe models which lie on the essentially the same fundamental plane.

As above, the MOND fundamental plane relation is sufficiently similar to the Newtonian virial relation that it can also be expressed in terms of a MOND FP mass (projected within $r_{eff}/2$) as a function of the dimensional mass unit $\sigma^2 r_{eff}/2G$. This is shown by the thick line in Fig. 1. This is the original ensemble of 360 anisotropic, polytropic models covering the range described above. We see that it is almost coincident with the observations of Bolton et al.

We may also apply the MOND fundamental plane relation in order to calculate the mass of a lens galaxy, projected within $r_{eff}/2$, from the observed velocity dispersion and effective radius. This calculated MOND FP mass is plotted against the observed lensing mass in Fig. 2. It is evident that the MOND FP mass is closely proportional to the lens mass, but about 30% less on average. This is understandable because the MOND FP mass is the total projected baryonic mass; the lensing mass, however, includes a pseudo-dark matter contribution because MOND, or its relativistic extension, TeVeS (Bekenstein 2004), provides extra deflection along the line-of-sight (Mortlock & Turner 2001; Zhao et al. 2006).

It is of interest to compare the MOND M/L values with population synthesis models. In Fig. 3 (lower panel) the indicated M/L values within $r_{eff}/2$ are plotted against $r - i$ colour and compared to the theoretical models of Bell et al. (2003). The luminosities have been determined from the

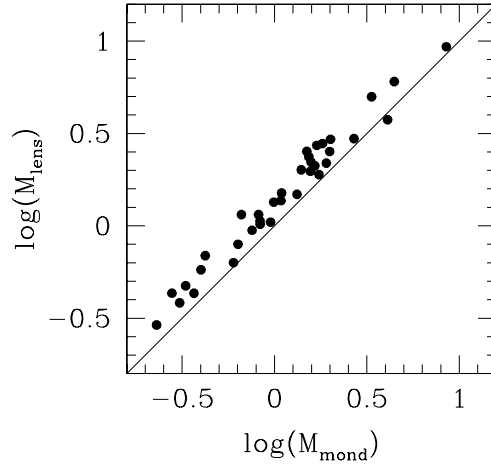


Figure 2. The logarithm of the observed lensing mass at $r_{eff}/2$ (Bolton et al. 2007) plotted against the logarithm of the projected MOND FP mass within $r_{eff}/2$ calculated via the MOND fundamental plane, eq. 5 (Sanders 2000). The solid line is the line of equality. The 30% offset is obvious.

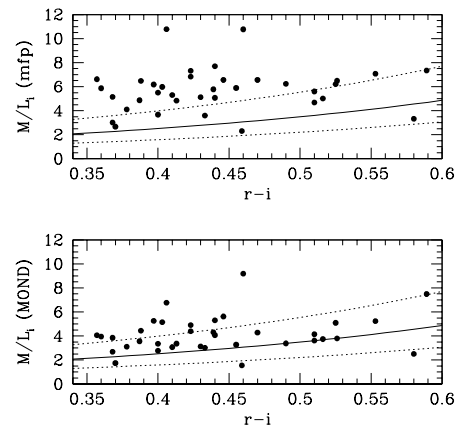


Figure 3. The upper panel shows the observed lensing M/L within $r_{eff}/2$ in the r band plotted against the $r - i$ colour. The solid line is the prediction of the population synthesis models of Bell et al. 2004 with the Kennecut or Kroupa initial mass function. The dashed lines show the 0.2 dex range which is a realistic estimate in the uncertainty of the estimated stellar M/L values given the uncertainty of the initial mass function and the effects of metallicity. The lower panel is the same for the MOND M/L.

observed Sloan magnitudes applying both K- and evolutionary corrections (Poggianti 1997) and reduced by a factor of about three to correspond to that within $r_{eff}/2$. We see that MOND M/L values closely track the theoretical values. The upper panel is the same except that the M/L is that determined from the projected lensing mass. Again the same trend is present although the offset discussed above is evident. In the context of MOND, this offset can be understood in terms of the extra deflection of photons by modified gravity along the line-of-sight— a deflection that can be interpreted as arising from phantom dark matter.

4 THE CONTRIBUTION OF MODIFIED GRAVITY TO THE DEFLECTION OF PHOTONS

The current multi-field relativistic extensions of MOND, such as TeVeS, are characterised by a physical metric which is distinct from the Einstein, or gravitational, metric. The transformation between the two metrics is “disformal” and chosen such that the relationship between the total weak field gravitational force and the deflection of photons is identical to that of General Relativity; specifically, the deflection angle is given by

$$\alpha = \frac{2}{c^2} \int g_{\perp} dz \quad (6)$$

where the integral is along the line of sight and g_{\perp} is the perpendicular component of gravitational force. The gravitational force includes not only the traditional Newtonian force but also an additional ‘MOND’ force (mediated by a scalar field) which becomes dominant at low accelerations.

This MOND force may be viewed as arising from a phantom dark halo. The phantom halo begins to make a significant contribution to the gravitational force and hence to the deflection of photons near the MOND transition radius

$$r_t = \sqrt{GM/a_0} \quad (7)$$

where M is the true (baryonic) mass of the object. In fact, the phantom halo may exhibit an apparent shell of matter between $1/2 r_t$ up to r_t depending upon the form of the function which interpolates between the MOND regime and the Newtonian regime (Milgrom & Sanders 2008). The relevance for the present discussion is that we would expect to find some evidence of “dark matter” in strong gravitational lensing if the Einstein ring radius is a significant fraction of the MOND transition radius; the larger that fraction, the larger the apparent contribution of dark matter to the projected mass detected by strong gravitational lensing.

The Einstein ring radius, for a point mass, is given by

$$r_{ein} = \frac{4GM}{c^2} \frac{D_l D_{ls}}{D_s} \quad (8)$$

where D_l , D_s , and D_{ls} are respectively the angular size distances from the observer to the lens, to the source and from the lens to the source. Combining eqs. 7 and 8 and making use of the fact that $a_0 = f c H_0$ where $f \approx 1/6$ we find that

$$r_{ein} = r_t F(z_l, z_s) \quad (9)$$

where F is a function of the lens and source redshift and depends upon the cosmological model.

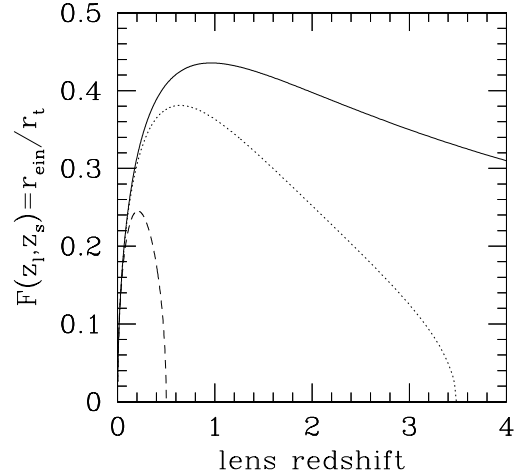


Figure 4. The Einstein radius in terms of the MOND transition radius as a function of the lens redshift for three different values of the source redshift: $z_s = 0.5$ (dashed curve), 3.5 (dotted), 100 (solid). This is for the standard “concordance” cosmology.

This function $F(z_l, z_s)$ is shown in Fig. 4 as a function of z_l for three different values of the source redshift ($z_s = 0.5, 3.5, 100$). This is all done for the standard “concordance” cosmology which the relativistic MOND cosmology should mimic to a close approximation. For the lenses in the sample of Bolton et al., $z_s \approx 0.5$ and $z_l \approx 0.2$ on average; therefore, F does not exceed about 0.25, and we might expect the contribution of an apparent halo to lensing to be relatively small. On the other hand for strong lenses considered by Treu & Koopmans (2004), $z_l \approx 1$ and $z_s \approx 3.5$ implying $F \approx 0.4$. The expectation is that there should be evidence for more “dark matter” in these high redshift systems, as, in fact, is reported by Treu & Koopmans.

We have estimated the contribution of modified gravity to lensing, in the form of projected phantom dark matter, for all of the objects in the sample of Bolton et al. The objects have been modelled as isotropic Jaffe spheres with the observed effective radius. Given this density distribution, the Jeans equation is solved for the run of radial velocity dispersion where the total force, g is related to the Newtonian force, g_N , by the MOND formula $g\mu(g) = g_N$; $\mu(x)$ is the MOND interpolating function ($\mu(x) = x$ where $x \ll 1$ and $\mu(x) = 1$ where $x \gg 1$), taken here to be of the form suggested by Zhao & Famaey (2006). In each case we adjust the mass of the sphere in order to reproduce the observed luminosity-weighted average line-of-sight velocity within $r_{eff}/2$; this mass in most cases agrees closely with that implied by the MOND fundamental plane (eq. 5). The difference between total (MOND) acceleration and the Newtonian acceleration ($|g - g_N|$) then allows us estimate the density distribution of the phantom dark halo. The projected MOND FP mass (X-axis in Fig. 2), presumably the visible mass of the galaxy, is then “corrected” by adding in the projected phantom dark mass. The result is shown in

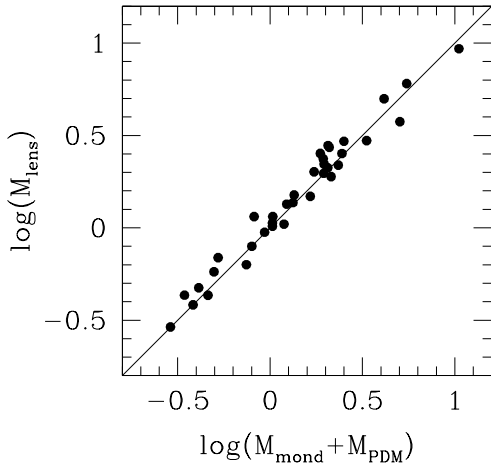


Figure 5. The observed lensing mass within $r_{eff}/2$ from Bolton et al. plotted against the projected MOND FP mass including the contribution of phantom dark matter (M_{PDM}). This corrects Fig. 2 for the effect of modified gravity on gravitational lensing.

Fig 5 which again shows the lensing mass vs. the MOND FP mass including the phantom dark matter. We see that a lensing mass which is 30% higher than the MOND mass is explained by the contribution of modified gravity to photon deflection.

We should note, however, that the Zhao-Famaey interpolating function favours the appearance of phantom dark mass within the optical image of the galaxy. This is because the transition from Newton to MOND is rather more gradual than for the often assumed ('standard') form of μ applied to calculation of galaxy rotation curves ($\mu(x) = x/\sqrt{1+x^2}$). Applying the standard form would result in a 10% reduction in the projected phantom dark mass, so the appearance of Fig. 5, and the conclusions we draw from it, would not be altered.

5 CONCLUSIONS

With MOND, the baryonic mass-rotation velocity relation for spiral galaxies, which forms the basis of the Tully-Fisher law, is exact in so far as it relates to the asymptotic rotation velocity measured far from the luminous galaxy. On the other hand, the mass-velocity dispersion relation for pressure supported systems, the basis of the Faber-Jackson law, is only exact for homologous models; the scaling of the relation depends upon the detailed characteristics of the object. Actual elliptical galaxies exhibit a range of properties— various shapes, varying degrees of deviation from an isothermal state and, no doubt, isotropy of the velocity dispersion— and cannot be represented by a single homologous sequence of models. Therefore, spheroidal galaxies will inevitably present a Faber-Jackson law with considerable scatter. None-the-less, MOND provides an explanation for

the remarkable fact that self-gravitating, pressure-supported quasi-isothermal objects with a velocity dispersion of a few hundred km s^{-1} will have a mass in the range of galaxies— or objects with a velocity dispersion $< 10 \text{ km s}^{-1}$ will have the mass of globular clusters— or objects with 1000 km s^{-1} will have the mass of a cluster of galaxies.

In spite of the scatter in the mass-velocity dispersion relation, when an additional parameter is added, such as effective radius or surface brightness, MOND models for elliptical galaxies define a narrow fundamental plane which is close, but not exactly equivalent, to that implied by the Newtonian virial relation for homologous objects. This was not part of the original set of MOND predictions but became apparent when it was realized that normal elliptical galaxies are essentially Newtonian systems within the effective radius and exhibit a wide dispersion in the effective radius-velocity dispersion relation. The properties of this fundamental plane were outlined by a set of 360 high order polytropic spheres with radially dependent anisotropy chosen to match the observed joint distribution of ellipticals by effective radius and velocity dispersion (Sanders 2000). Applying this fundamental plane relation to determine the mass of those ellipticals in the sample of Jørgenson et al. (1995) yielded reasonable values for the mass-to-light ratios.

Now, thanks to the work of Bolton et al. (2007) we can compare this mass-based MOND fundamental plane directly to the observed mass-based fundamental plane as defined by this set of 36 strong gravitational lenses. Figs. 1 and 2 illustrate that the two coincide apart from a systematic offset of about 30%. Indeed, the implied MOND mass-to-light ratios are completely consistent with population synthesis models (Fig. 3), and the small discrepancy between the lensing mass and the MOND FP mass can be understood in terms of the contribution of modified gravity to the deflection of photons (Fig. 5). It is important to recall that the properties of the MOND fundamental plane (Sanders 2000) were defined well before those of observed mass-based fundamental plane (Bolton et al. 2007) so this does, properly speaking, constitute a prediction that has been subsequently confirmed.

Most significantly, there is no evidence from strong gravitational lensing for a significant mass discrepancy within these high surface density systems— as MOND would robustly predict. This is in contrast to a recent claim by Ferreras et al. (2008) based upon lensing by six early type galaxies. They note that the lensing mass, as determined either by General Relativity or MOND (as extended by TeVeS), is significantly greater than the stellar mass estimated via population synthesis models. However, this conclusion appears to give much weight to the precision of such models; the mass difference is generally smaller than the differences due to the assumption of different initial mass functions ($\approx 0.2 - 0.3$ dex). Moreover, in the near infrared, the scatter induced by metallicity effects can be comparable (Bell et al. 2003). Overall it is difficult to argue that implied mass-to-light ratios ranging from two to eight constitute compelling evidence for dark matter in early-type galaxies.

The conclusions here are generally consistent with those of Zhao et al. (2006). Looking at a sample of 18 strong double-image lenses from the CASTLES sample in the context of TeVeS, they concluded that the implied lensing masses are consistent with the observed baryonic matter (with additional deflection provided by the modified grav-

ity). There are two extreme outliers, but this is not unsurprising in view of the possible contribution of surrounding groups or clusters to deflection of photons (in one case, the implied lensing mass is significantly less than the estimated stellar mass which would also be a problem for GR). Treu & Koopmans (2004) have argued for the presence of a significant fraction of dark matter ($f_{DM} = 0.3 - 0.7$) within the Einstein ring radius of five well-observed high redshift lens systems (for the systems considered in this paper interpreted in terms of dark matter $f_{DM} = 0 - 0.4$). We have argued that such a result is expected because of the larger contribution of modified gravity to the deflection of photons in higher redshift systems where the Einstein ring radius is a larger fraction of the MOND transition radius (Fig. 4).

The results here for this homogeneous relatively nearby sample of lenses are encouraging for MOND— both with respect to the confirming the MOND fundamental plane and to the basic prediction of small discrepancy in high surface density systems. Such observations clearly constitute a powerful test of MOND as an acceleration based modification. A single case of an isolated HSB galaxy showing a large discrepancy within the bright regions, would be problematic for the theory.

We thank Lèon Koopmans and Adam Bolton for sharing the data on the SLACS gravitational lenses. We are also very grateful to Lèon and to Moti Milgrom for helpful comments on the initial manuscript.

REFERENCES

- Bekenstein J.D., 2004, *Phys.Rev.D*, 70, 083509
 Bekenstein J.D., Milgrom M., 1984, *ApJ*, 286, 7
 Bell E.F., McIntosh D.H., Katz N., Weinberg M.D., 2003, *ApJS*, 149, 289
 Benardi M., et al., 2003, *AJ*, 125, 1866
 Binney J., Tremaine S., 1987, *Galactic Dynamics*, Princeton Univ. Press, Princeton, N.J.
 Bolton A.S., Burles S., Treu T., Koopmans L.V.E., Moustakas L.A., 2007, *ApJ*, 665, L105
 Djorgovsky S., Davis M., 1987, *ApJ*, 313, 59
 Dressler A., Lynden-Bell D., Burstein D., Davies R.L., Faber S.M., Terlevich R., Wegner G., 1987, *ApJ*, 313, 42
 Ferreras I., Sakellariadou M., Yusaf M.F., 2008, *Phys.Rev.Lett.*, 100, 031302, arXiv:0709.3189
 Jaffe W., 1983, *MNRAS*, 202, 995
 Jørgensen, I. *MNRAS*, 1999, 306, 607
 Jørgensen, I., Franx, M. & Kærgard, P. 1995a, *MNRAS*, 273, 1097
 Jørgensen, I., Franx, M. & Kærgard, P. 1995b, *MNRAS*, 276, 1341
 Kochanek C.S., Schneider P., Wambsganss J., 2004, Part 2 of *Gravitational Lensing: Strong, Weak & Micro*, Proc. 33rd Saas-Fee Advanced Course, G. Meylan, P. Jetzer & P. North, eds. (Springer-Verlag: Berlin)
 Milgrom M., 1983, *ApJ*, 270, 365
 Milgrom M., 1984, *ApJ*, 287, 571
 Milgrom M., Sanders R.H., 2003, *ApJ*, 599, L25
 Milgrom M., Sanders R.H., 2008, *ApJ* (in press), arXiv:0709.2561
 Mortlock D.J., Turner E.L. 2001, *MNRAS*, 327, 557
 Pryor C., McClure R.D., Fletcher J.M., Hesser J.E., 1989, *AJ*, 98, 596
 Poggianti B.M., 1997, *A&A Suppl.*, 122, 399
 Romanowsky A.J., et al., 2003, *Science*, 301, 1696
 Sanders R.H., 2000, *MNRAS*, 313, 767
 Sanders R.H., 2008, *MNRAS* (in press), arXiv:0712.2576
 Treu T., Koopmans L.V.E., 2004, *ApJ*, 611, 739
 Zhao H.-S., Bacon D.J., Taylor A.N., Horne K., 2006, *MNRAS*, 368, 171
 Zhao H.S., Famaey B., 2006, *ApJ*, 638, L9